Hindawi
Journal of Computer Networks and Communications
Volume 2019, Article ID 2938653, 11 pages
https://doi.org/10.1155/2019/2938653

Research Article

Adaptive Filtering in Optical Coherent Flexible Bit-Rate Receivers in the Presence of State-of-Polarization Transients and Colored Noise

Ahmad Abdo and Claude D'Amours

School of Electrical Engineering and Computer Science, The University of Ottawa, Ottawa, Ontario K1N6N5, Canada

Correspondence should be addressed to Ahmad Abdo; aabdo013@uottawa.ca

Received 29 July 2019; Revised 18 September 2019; Accepted 10 October 2019; Published 3 November 2019

Academic Editor: Youyun Xu

In this article, we analyze the performance of adaptive filtering in the context of dual-polarization coherent optical flexible bit-rate transceivers. We investigate the ability of different adaptive algorithms to track fast state-of-polarization (SOP) transients in the presence of colored noise. Colored noise exists due to the concatenation of Wavelength Selective Switches (WSSs) and polarization dependent loss (PDL) which can be considered as spatially dependent noise. We consider the use of different modulation formats, and the practical limitation of error signal feedback delay in decision-directed adaptive filters is also taken into account. The back-to-back required signal-to-noise ratio (RSNR) penalty that can be tolerated determines the maximum SOP rate of change that can be tracked by the adaptive filters as well as the filter's adaptive step size. We show that the recursive least squares algorithm, using the covariance matrix as an aggressive "step size," has a much better convergence speed compared to the least mean squares (LMS) and normalized LMS (NLMS) algorithms in the presence of colored noise in the fiber. However, the three algorithms have similar tracking capabilities in the absence of colored noise.

1. Introduction

The era of cloud-based computation has arrived. To be able to accommodate the increased data rates and increased number of communicating devices on the internet, new techniques in optical telecommunications are being developed. The main vehicles for high-capacity networks are flexible bit-rate transceivers that use coherent detection and dual polarization. Dual polarization, introduced in [1], effectively doubles the data rate compared to single polarization techniques. The core operator in dual-polarization communication systems is the adaptive filter which performs equalization to correct the time-varying state-of-polarization (SOP) as well as other linear channel impairments. Studying both the convergence and tracking performance of the adaptive filters used in this process is important in understanding the limitations of the system.

The linear impairments encountered in an optical channel are a mix of deterministic and stochastic impairments. Chromatic dispersion (CD) is a type of deterministic impairment while polarization mode dispersion (PMD), polarization dependent loss (PDL), and SOP are stochastic ones. A dual-polarization optical signal has amplitude and phase in one polarization (X) and another amplitude and phase in the orthogonal polarization (Y). The received optical signal is a rotated version of the transmitted one. The rotation caused by the channel is either static or slowly varying which allows the receiver to employ a linear adaptive filter to decouple the two polarizations from the received rotated optical signal. Algorithms such as the classical least mean squares (LMS) [2–4] and the constant modulus algorithm (CMA) [5] have been used to undo the effects of the channel rotation.

In this paper, we investigate the performance of the LMS, normalized LMS (NLMS), RLS, and MMA algorithms for the adaptive filter in coherent receivers for dual-polarization optical signals in the presence of SOP transients, PDL, and optical filters. Then, we provide an overview of the main sources of SOP transients in optical links. In the next section,

we look at the related literature discoursing adaptive filtering in coherent receivers. We present the concept of flexible bit-rate transponders in emerging programmable optical networks. In Section 5, we present a theoretical overview of coherent receivers and adaptive filtering. The simulation environment details are given, and then, we present our simulation results where we focus on the effect of SOP rate of change on RSNR penalty, as well as the tradeoff between performance in back-to-back (i.e., patch cord fiber between the transmitter and receiver) link configuration versus PDL penalty versus SOP tracking capabilities. As well, we compare different adaptive algorithms by simulating their convergence speed and SNR penalty for different SOP transients' speed. The main contributions of this paper are the following:

(1) Study of SOP tracking in the context of flexible bit-rate optical transceivers with practical hardware limitation

(2) Illustrating the tradeoff when equalizing static versus fast variant channel, i.e., back-to-back RSNR and PDL penalties versus SOP tracking penalty.

(3) Presenting analysis and simulation, in both convergence and steady states, to compare the performance of LMS versus NLMS, MMA, and RLS in the presence of colored noise (PDL and Filtering) and SOP transients

The work presented in this paper is an extension of the work presented in [6]. The work presented in [6] focuses on the RSNR penalty when the LMS algorithm is used to correct for SOP, PDL, and ROADM filtering effects in dual-polarized networks using QPSK modulation. The data rate is fixed, and the results are presented as an RNSR penalty for a given SOP rate and PDL level. In this work, we consider the performance of different adaptive filtering algorithms for the correction of SOP transients, PDL, and ROADM filtering effects in flexible bit-rate transceivers in software-defined networks which employ different modulation formats (QPSK as well as MQAM, where $M = 8$, 16, 32, and 64). The results are presented in terms of maximum SOP rates that can be tracked by the different algorithms for a given RSNR penalty and for different levels of PDL and number of ROADMs. Therefore, this work is a much more comprehensive study of the use of adaptive filters in dual-polarized coherent networks in the presence of fast SOP transients, PDL, and ROADM filtering effects than [6].

2. Causes of State-of-Polarization Transients

Optical ground wires (OPGW) are primarily deployed by the electrical utility industry. They shield the conductors from lightning strikes, while providing a telecommunications path for third party communications. High-voltage lines carry electricity from the utility to the consumers while fiber optic cables provide telecommunication capability. OPGWs are being increasingly deployed to reduce costs compared with buried fibers; however, lightning strikes and other phenomena can cause the transmitted data to be exposed to fast SOP transients. In [7], it is stated that a 100 km length of OPGW can experience roughly 30 lightning strikes per year in Central Europe. The external structure of OPGW is constructed to discharge the lightning, but the Faraday effect, [8], is observed on the two polarizations when a lightning strike occurs.

An in-depth study performed using Verizon aerial fiber in [9, 10] showed that aerial fibers typically encounter higher SOP transients than those buried in the ground. In [11], data were collected from an OPGW plant in order to determine the correlation between SOP transients and lightning strikes. They were able to demonstrate a high correlation between lightning strikes and the occurrence of fast SOP transients which could achieve rates of up to 5.1 mrads/sec. Laboratory experiments were conducted in [12, 13] to emulate the effect of lightning on SOP transients observed in OPGW fibers. They showed that the rate of change in SOP increases as both the electrical current created by the lightning strike and the length of the cable increases. They demonstrated through repeated trials that for a given lightning current and cable length, the variance of the measured SOP data was less than 0.5% about the mean. In [14], the authors report that wind speed and the high-voltage line current also have an effect on the SOP rate of change.

Temperature and other forces can also have an effect on SOP in fiber cables. For example, deep sea cables experience mean SOP variations of 200 Hz, [15], while the mean SOP rate of change is 50 Hz in submarine cables, as shown in [15]. The authors of [16] found that the rate of SOP change is correlated to variations in ambient temperature. Other causes of fast SOP variation are mechanical vibration of the fiber cable caused by the passage of trains or construction work in close proximity. In [17], a study of SOP induced by mechanical vibration of Dispersion Slope Compensation (DSC) modules was done. The special case about DSCs is that they contain long fibers that are typically meant to compensate for dispersion of a span of the DWDM network (80 km). Certain packaging methodologies were introduced in [18] to reduce the fluctuations of SOP in DSC modules.

Much work has been done on reducing the RSNR penalty to compensate for the different impairments that are typical in coherent dual-polarization communication systems over fiber cables. In [19], it was shown that PMD actually helps averaging the penalty due to PDL. This is due to the fact that PMD spreads both polarizations equally at the two extreme PDL axes of the fiber. In [20], coding on the X and Y polarizations is used to mitigate PDL to avoid worst case orientations, which in turn reduces the RSNR penalty due to PDL. However, neither study considered the effect of fast SOP transients.

3. Overview of Adaptive Filters in Optical Coherent Receivers

In [21], the authors presented a field-programmable gate array implementation of a coherent dual-polarization receiver where quadrature phase shift keying (QPSK) modulation is used. Operating at a data rate of 2.8 Gb/s, their receiver's adaptive filter was able to track SOP transients of

5 kHz in the presence of 3 dB PDL in the link with a RSNR penalty of 0.5 dB. The work in [22] compared LMS algorithm with the recursive least square (RLS) algorithm in a system that employs spatial-division multiplexing (SDM), where multiple modes travel in the fiber in order to increase channel capacity. They show that the RLS has the superior convergence properties. The authors of [23] considered the effects of error feedback delay, using CMA, on the performance of the coherent receiver in the presence of CD. The work done in [24] shows how pipelining and efficient implementation of the adaptive filter's feedback loop in the receiver help reducing the delay of the error signal used in the LMS tap weight updates by 18%.

In [25], the authors looked at Kalman filtering to tracking SOP with some PDL and frequency offset. Beside the fact that Kalman requires processing complexity in the order O (N^3), which does not fit in the industry's trend to reduce power consumption in optical transceivers, there are two issues: conversion from Jones to Stokes parameters introduces noise enhancement in fixed-point implementation and the prerequisite for a fiber model in order to get the prediction and then compare with measurement for correction makes it tough to generalize. Constant Amplitude Zero Auto-Correlation (CAZAC) sequence, [26], are popular in wireless studies, and they are used in long-term evolution (LTE). In [27], the authors performed a detailed study on the impact of CAZAC in a long-haul transmission system viewed as chirp signals. In the studies undertaken in [28, 29], frequency-domain equalization (FDE) is used to track the SOP transients, using only QPSK modulation, in the pilot-directed mode. The papers focused on the amount of averaging of the channel estimates in tradeoff of back-to-back penalty and SOP transients tracking. The authors in [28–30] did not consider other types of optical fiber impairments such as PDL and optical filtering.

4. Flexible Bit-Rate Transceivers in Software-Defined Networks

Next generation coherent receivers are designed to support high-speed, reduction in power consumption, and flexible provisioning. They are an integral component in the migration to Software-Defined Networks [31]. The programmability is required so that network operators can switch between modulation formats, to support flexible bit-rates based on reach, optical link margin, and available spectrum bandwidth. Therefore, it is worth studying the performance of the adaptive filters with the same practical limitations for different constellations (different line rates). We consider QPSK and 16QAM as high-order modulation format deployed for long reach link, throughout most of the study. As well, we look at the SOP rate of change tracking, for a different SNR penalty, of LMS for QPSK and 8/16/32/64 QAM. The PDL values, associated with modulation formats shown in Figure 1, are estimates based on the possible number of spans per bit-rate.

In a typical link-budgeting process, operators and equipment vendors include SNR margin when planning optical networks [32]. Examples of the reasons for the unused what we call "Fiber Link SNR Margin" are to account for laser aging, amplifier power transients, pixels drift in ROADMs, and fast SOP transients. The trends in standardization bodies such as IEEE802.3/OIF are focusing on, among other things, Soft-Decoding Forward Error Correction (FEC) with high threshold (in [33], FEC threshold used is 4.5×10^{-2} with 24% overhead for 64QAM modulation format and a propagation scenario of 300 km). Therefore, we chose the FEC threshold that will define our operating point with base SNR at 4.5×10^{-2} for all modulation formats studied:

$$\text{Link SNR} = \text{SNR}(@\,\text{BER} = 4.5\%) + \text{Fiber Link SNR Margin}. \quad (1)$$

Adaptive filtering methods, such as LMS, are the core elements in the design of the coherent receivers. LMS converges toward the Weiner solution [3], and implementation can be in time domain or frequency domain [34]. Since the error calculated in decision-directed modes are part of the update equations, the availability of the error vector is key to making the right update to compensate for the time-varying channel impairments. The two main time-varying impairments we will consider are fast SOP transients and PDL. The former is usually illustrated on the Poincaré sphere and modelled mathematically as changes in the Stokes vector representation. The instantaneous PDL, resulting from contributions of many random birefringences in fibers and optical components along the link, can be chosen from the Maxwell distribution [35]. It is considered a time-varying impairment where one of the received polarizations is attenuated in a random fashion. A typical digital signal processor in a coherent receiver contains static and adaptive filters, carrier phase/frequency recovery as detailed in [36], and a threshold-based decision block. For adaptive filter algorithms to work in the data-directed mode, the error is measured at the output of the decision block. Signal processing operates at much slower speed than the sampling rate. As the modulation order increases, the complexity of the carrier recovery algorithm and detector/decoder increases and results in increased feedback delay (FD) of the error signal used to update the filter tap weights. As part of the design, there will be tradeoffs between size, power, and amount of FD. The more parallelism in the implementation, i.e., processing more symbols at same time, the smaller the FD, but then the number of hardware gates is larger due to increased number of operations per Application-Specific Integrated Circuit (ASIC) clock, as shown in [37], and therefore, power consumption will be higher. In dual-polarization coherent detection, the adaptive filter can have one of the two configurations: 2×2 MIMO (Multiple Input Multiple Output) system equivalent to 4 independent filters where X and Y common impairment are compensated, or 4×4 MIMO [38, 39], at the price of more power consumption, that can compensate for X and Y, as well, in-phase and quadrature-related impairments such as delay and loss/gain imbalance. In the presence of FD in the adaptive filter loop, the update equation is modified where the current update is based on outdated input data r and error (ε) by FD

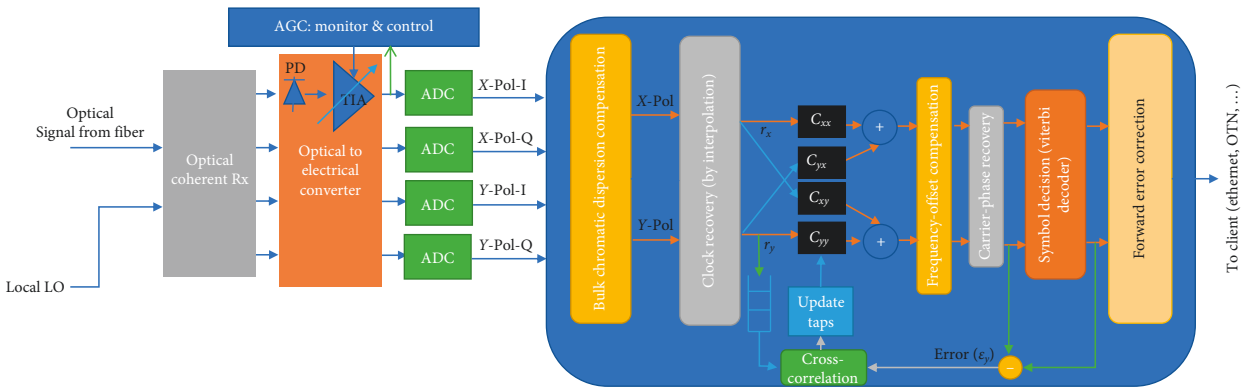

Figure 1: Typical architecture of a coherent receiver.

blocks. The larger the loop delay, the greater the lag error which results in limitations on stability and bandwidth. This reduces the maximum value for the adaptive filter step size which in turn limits the maximum rate of channel state variations that the adaptive filter can track. The main advantage of having the FIR (finite impulse response) operates per block of symbols is the reduction of computational complexity. Knowing that with baud rate equals to 80 Giga-Baud (GBaud), the symbol spacing is 12.5 ps. Assuming the requirement set by customers for the PMD handling of the coherent transponder to be peak of 200 ps and with adaptive equalizer operating at T (symbol period)/2 spacing, the FIR filter needs 32 taps per branch. A fractional equalizer with tap delays matched to the receiver bandwidth, or to the transmitted pulse shape (e.g., raised cosine), can help reduce ISI or channel distortion [40]. The ISI may be due to chromatic dispersion, PMD, channel multiplexers/demultiplexers, ROADMs, or nonideal transmitter or receiver responses. The waveform at the output of the transversal filter is

$$\text{Output}(t) = \sum_{i=0}^{N} C_i \cdot \text{Input}(t - t_i). \tag{2}$$

For LMS-based filters, with coefficients named $[C_{xx}, C_{yx}, C_{xy}, C_{yy}]$, the update algorithm can be expressed by the following equations when taking the feedback delay in consideration with subscript based on the polarization:

$$\begin{aligned} C_{xx}(n+1) &= C_{xx}(n) - \mu r^*_{x,n-\text{FD}} \varepsilon_{x,n-\text{FD}}, \\ C_{yx}(n+1) &= C_{yx}(n) - \mu r^*_{y,n-\text{FD}} \varepsilon_{x,n-\text{FD}}, \\ C_{xy}(n+1) &= C_{xy}(n) - \mu r^*_{x,n-\text{FD}} \varepsilon_{y,n-\text{FD}}, \\ C_{yy}(n+1) &= C_{yy}(n) - \mu r^*_{y,n-\text{FD}} \varepsilon_{y,n-\text{FD}}, \end{aligned} \tag{3}$$

where $\mathbf{C}$ is the coefficient of the adaptive filter, ε is the error signal fed back from the output of the decision circuit to use in the tap weight update, and r is the input signal buffered by FD blocks. For NLMS, the step size μ is normalized by the power of the 2×1 received Jones vector. The standard RLS adaptive algorithm considered in this paper is based on the update equations below:

$$\mathbf{C}_{\text{RLS}}(n+1) = \mathbf{C}_{\text{RLS}}(n) + \mathbf{P}(n) r_{n-\text{FD}} \varepsilon_{n-\text{FD}}, \tag{4}$$

$$\begin{aligned} \mathbf{P}(n+1) = {} & \frac{1}{\lambda + r(n)^T \mathbf{P}(n-1) r(n)} \\ & \cdot \left(\mathbf{P}(n) - \mathbf{P}(n) r(n) r(n)^T \mathbf{P} \right), \end{aligned} \tag{5}$$

where received signal r and error ε are 2×1 vectors and λ is the forgetting factor. $\mathbf{P}$ and $\mathbf{C}_{\text{RLS}}$ (same for LMS/NLMS) are 2×2 matrices, the latter representing all four FIRs:

$$\mathbf{C}_{\text{RLS}} = \begin{bmatrix} C_{xx} & C_{yx} \\ C_{xy} & C_{yy} \end{bmatrix}. \tag{6}$$

In the case of multimodulus algorithm (MMA), an upgrade of CMA for multilevel constellations, with r as the nearest constellation point measured at the output of the adaptive filter and the error functions are as follows:

$$\begin{aligned} \varepsilon_x &= \widehat{r^2} - \left| \widehat{y_x} \right|^2, \\ \varepsilon_y &= \widehat{r^2} - \left| \widehat{y_y} \right|^2. \end{aligned} \tag{7}$$

The filtered data per polarization going to the carrier recovery block is therefore a combination of two branches as shown below:

$$\begin{aligned} x_{\text{out}} &= C_{xx} \cdot r_x + C_{yx} \cdot r_y, \\ y_{\text{out}} &= C_{yy} \cdot r_y + C_{xy} \cdot r_x. \end{aligned} \tag{8}$$

The MMSE, minimum mean-square solution, or Wiener solution [3] will take this form when $\mathbf{H}$ is the frequency response of the channel and N_0 is the noise variance:

$$\mathbf{C}_{\text{opt}} = \left[\mathbf{H}^H \mathbf{H} + N_0 I \right]^{-1} \mathbf{H}^H, \tag{9}$$

$(.)^H$ and $(.)^{-1}$ are, respectively, Hermitian and inverse operators. PDL accumulates in a link mainly due to birefringent elements (mechanical stress or variability in the manufacturing process) and Wavelength Selective Switches (WSSs) [40]. The general Jones 2×2 matrix, with θ rotating with the rate indicated in the simulation results and Φ set to 0, is shown in the equation below:

$$\mathbf{H}_{\text{rotation only}} = \begin{bmatrix} \cos(\theta) \cdot \exp(i\Phi) & \sin(\theta) \cdot \exp(i\Phi) \\ -\sin(\theta) \cdot \exp(-i\Phi) & \cos(\theta) \cdot \exp(-i\Phi) \end{bmatrix}. \tag{10}$$

5. Simulation Methodology

PDL is typically simplified as one bulk random attenuator for one of the two polarizations. However, in the literature such as [41], the ingress and egress rotation matrices are modelled as being the same, which is not precise. The reason is that the PDL element is typically connected to fibers at the input/output, which implies different Jones rotation being applied. In this correspondence, our model has the two unitary matrices (represented by RI and RII), functions of θ and β, independent:

$$\mathbf{H}_{\text{channel}} = \underbrace{\begin{bmatrix} \cos(\theta) & \sin(\theta) \\ -\sin(\theta) & \cos(\theta) \end{bmatrix}}_{\text{RI}} \underbrace{\begin{bmatrix} 1 & 0 \\ 0 & k \end{bmatrix}}_{\text{PDL}} \underbrace{\begin{bmatrix} \cos(\beta) & \sin(\beta) \\ -\sin(\beta) & \cos(\beta) \end{bmatrix}}_{\text{RII}}. \tag{11}$$

where $0 < k < 1$. The attenuation in dB is as follows:

$$\text{PDL}_{\text{dB}} = -20 * \log_{10}(k). \tag{12}$$

Since θ and β are randomly varying, the two polarizations (X and Y) are mixed in a time-varying manner. It is up to the adaptive filter at the receiver to correct and track for the time-varying crosstalk effects. SOP of full 2π rotation on Poincaré sphere, as in Figure 2, was performed for each tested SOP rate of change. The high-level parameters used in the simulations are as follows: symbol rate of 33 GBaud, 11 complex taps per filter, and fixed block size of 512 symbols.

6. Simulation Results and Discussions

In this section, we present our simulation results based on the theory and assumptions above. We begin by showing the impact of adaptive filter step size on both back-to-back and PDL RSNR penalty versus the ability to track fast SOP transient. We will look at the limitation of feedback delay for different modulation formats. At the end, we compare different adaptive filtering methods in the presence of colored noise such as PDL.

6.1. Impact of Step Size on SNR and Tradeoffs in Presence of Feedback Delay. We know from [42] that large step size increases misadjustment errors, while small step size makes adaptation of taps prone to lag errors. As we see below, even in the back-to-back (B2B) condition, the SNR penalty increases as the function of step size. In our simulation, the taps are initialized to an 2×2 identity matrix. As we increase PDL, which causes more fluctuation in the measured SNR at the output of the adaptive filter (higher rate of the error), the slope of the SNR penalty gets higher. As error feedback delay increases, the lag error becomes more dominant in the adaptive loop. Also, as discussed above, when high step size is utilized, we amplify the distortion by misadjustment;

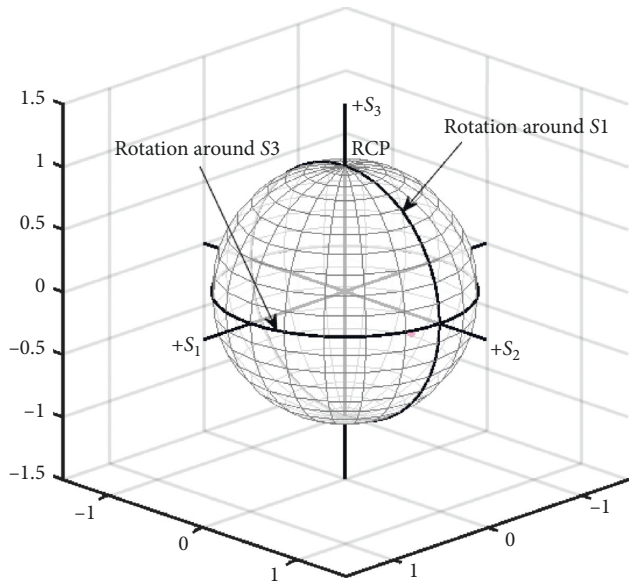

Figure 2: Poincare sphere illustrating different transient trajectories.

therefore, we get even more decision errors that will be translated into larger SNR penalty. Using high-order modulation formats, such as 16/32/64QAM, the decoding process becomes more complex, as well as carrier recovery circuits; therefore, FD is becoming larger in state-of-the-art coherent receivers. The new upper bound on the step size is a function of error signal feedback delay, and it is governed by the equation below (here, FD starting index is 0) [43]:

$$0 < \mu < \frac{2}{\lambda_{\max}} * \sin\frac{\pi}{2(2 * \text{FD} + 1)}. \tag{13}$$

A shown in Figure 3, for 16QAM, there is a tradeoff between B2B/PDL RSNR penalty versus SOP rate of change tracking. The smaller the step size, the more stable the adaptive filter; however, the slower it is to adjust the directions of the taps to track the changes in the state of polarization. On the other hand, the larger the step size the faster the adaptation rate. It is shown as well that the SNR Margin (2 and 6 dB) on the link does not make much of a difference in presence of large feedback delay (FD). We compared the results of data-directed (DD) to 16 symbols pilot-directed (PD), equivalent to 5% overhead, and the latter by default has a FD of 1 since the symbols are known to the receiver and there is no need to get feedback to measure the error. However, if no averaging is performed on multiple measures of the received pilot symbols, the SNR penalty is high due to noisy estimates. On the other hand, as expected due to small delay as shown in "PD | FD = 1 | Fiber SNR Margin = 4 dB," the tracking speed of CAZAC-based PD is higher than tracking capability of DD.

In [29], SOP-related tracking capability is studied, and the authors used CAZAC-based frequency-domain zero-forcing and minimum mean-square error to get channel estimation. As well, with feedback delay set to larger value (as performing more averaging on training symbols), the

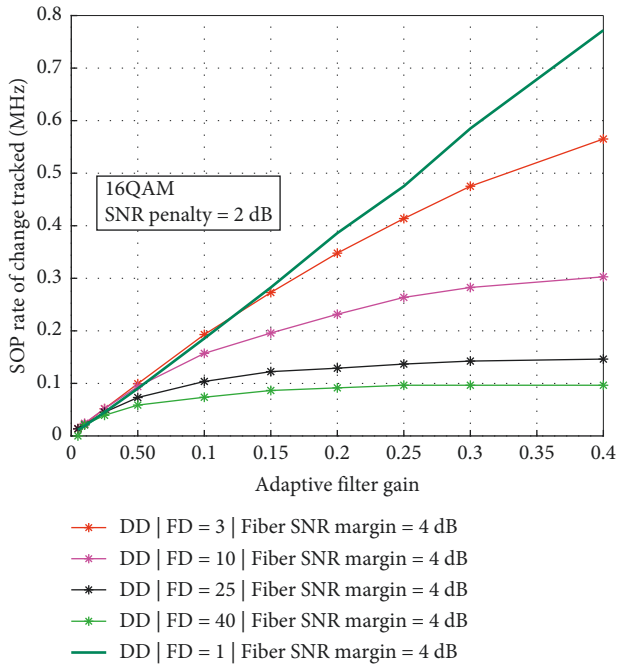

Figure 3: Maximum SOP versus LMS gain (i.e., step size) using 16QAM.

maximum SOP tracking capability for a fixed penalty is reduced. It is known that DD has much lower back-to-back penalty and, for same SNR penalty, higher SOP tracking when FD is set to 1. The reason is that in DD, there are more data available to tune the coefficients, unlike PD where only 16 data points are used. The SNR penalty of PD can be reduced by performing more averaging of multiple received training symbols, before updating filtering coefficients, especially when operating in OSNR link (i.e., noisy channel).

One way to increase spectral efficiencies in optical fiber links is to increase the baud rate, i.e., symbol rate. With new CMOS technologies, such as 16 nm [44], new high-speed data converters working at 80 and 100 GBaud, as shown in [45, 46] respectively, are implemented in products nowadays. That will be converted to higher ASIC clock and faster signal processing and therefore faster convergence and more tracking of change in SOP transients. Clock speed that is driving the adaptive filter and other functionalities in the ASIC is an important factor that determines the amount of SOP tracking, as well as in [47], if buffering of incoming data is used and then SOP rotation feed-forward correction is performed, then the SNR penalty can be reduced, and SOP tracking tolerance increased. In [48, 49], the authors introduced a method to choose variable step size per coefficient based on the feedback error or link SNR. Such method will help reducing the tradeoff between misadjustment and tracking ability of the fixed step size.

6.2. SNR Penalty versus SOP Transients. To avoid disturbing traffic, network operators design their dense-wavelength division multiplexing links with some OSNR margin (typical 3 to 4 dB). It is reflected in their link budget to account, as shown in [50], for SOP transients and for end-of-life-related performance degradations such as lasers drift, center frequencies per port drift of link filtering, and changes in transfer functions of electro-optical components. Increasing the LMS gain and the SOP tracking penalty introduces a noise penalty and not an OSNR penalty. It is not correct to use OSNR penalty (in dB) as a comparator because it unfairly disadvantages any modulation format that has a higher back-to-back RSNR. As described in [51], higher order constellations are more sensitive to noise. Therefore, noise penalty is the relevant figure of merit for comparison for different modulation formats and baud-rates. However, for the sake of performing comparison with a metric that is used in typical link budget planning tools, we will use SNR penalty (and not Optical-SNR, which takes into consideration the bandwidth of the signal versus the 12.5 GHz noise bandwidth), while the noise can be retrieved as follows:

$$\text{Noise}_{\text{dB}} = -10 * \log_{10}\left(10^{-(\text{RSNR}_{\text{base}}/10)} - 10^{-(\text{RSNR}_{\text{impaired}}/10)}\right). \quad (14)$$

Another source of impairments in optical links is the filtering effects of the concatenation of ROADMs. They are based on Wavelength Selective Switches (WSS) and can be silicon-based as presented in [52]. To study the impact of filtering on SOP tracking, we used the fiber model in Figure 4. Noise was added for each span as it is the case in real optical links. The simulated data stream was shaped at the transmitter with Root-Raised Cosine (RRC) pulse shaped to comply with zero ISI criterion since the bandwidth is limited. The set rolloff factor chosen was 0.21, along with the mentioned baud rate of 33 GBaud, and the total bandwidth of the signal is 40 GHz. Considering it is 16QAM, it allows a line rate of 264 Gb/s (33 (GBaud) $*$ 4 (dual polarization) $*$ 2 (bits per baud)) without consideration of forward error control (FEC) overhead. We tested one set of filters, combined with the transfer function of the common multiplexer/demultiplexer, to mimic 12 spans (have 6 ROADMs) optical link, with resulting effective 3-dB bandwidth of 37.3 GHz.

As the rate of SOP increases, the penalty gets higher. For 12 spans/PDL = 6 dB versus PDL = 6 dB only, the penalty for SOP at 20 kHz is 0.2 dB while it is 0.4 dB at 25 kHz. Based on some fitting on the data in Figure 5, for each one dB PDL increase in a fiber link, the capability of tracking of SOP is reduced by 7.1 kHz and 8.6 kHz for SNR penalty of 1 and 2 dB, respectively. As well, a bulk PMD of 10 picoseconds does not have major impact on the tracking speed for a given SNR penalty (<0.4 dB). However, in a distributed system where PMD and PDL interplay, as shown in [18], it is expected that PMD will help distributing the PDL loss equally to the two polarizations. Therefore, the impact of PMD will be even smaller. It is worth noting that in real fiber link with many filtering sites, the variability in the BER gets higher since the PDL of the link is fluctuating over time. Our observations showed that the adaptive filter taps are noisier due to increase in the feedback error during the transient; therefore, the estimate even of the static portion of the fiber

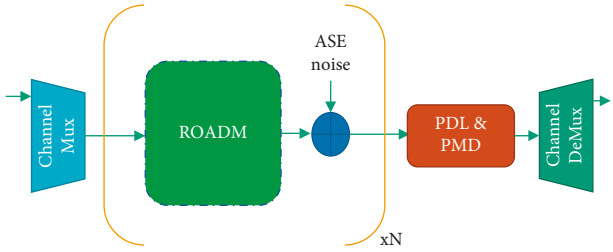

Figure 4: Simulated fiber model.

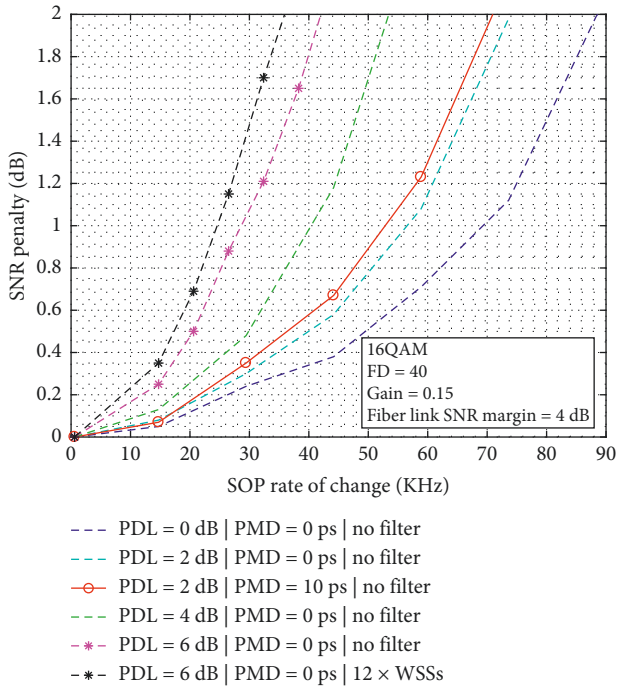

Figure 5: Penalty of SOP tracking for 16QAM for different PDLs.

channel will be noisy and hence higher the penalty. As well, the BER variability gets higher as PDL increases, and it is mainly due to upsurge in randomness of attenuation and SNR measured per polarization. Therefore, the maximum LMS step size required to assure stability gets smaller. In Figure 5, we scaled all penalties to remove base due to the additional impairment; therefore, at 0 kHz SOP transient, the penalties associated are "0." As shown, the penalty increases when adding the 12 spans model to the PDL, which is due to the receiver signal having its high frequency components attenuated by the filtering. When LMS tries to recover the data, it boosts noise as well and hence the increase in the Bit Error Rate (BER).

6.3. Tracking Transients for Different Modulation Formats. With programmable transponders being the norm in next generation Software-Defined Networks, the same hardware will be used for supporting the transmission of more than one modulation format. Therefore, it is important to study SOP tracking capabilities of one modem for various line rates. It is safe to assume that the feedback delay is the same for different modulation formats to reduce hardware footprint/complexity. As we see below, the maximum achievable SOP tracking gets smaller when the modulation order is higher. The reason is that the Euclidian distance between nearest points is smaller for higher order modulation constellations and, as described in [51], for wireless applications, high-order constellations are more sensitive to even modest amount of added noise. For different measured SNR penalties and "Fiber Link SNR Margin" set to 4 dB, we show, in Figure 6, the reduction in SOP tracking capability as the number of bits per symbol increases. In the case of SOP transients, an untracked change in the state of polarization rotates vectors on the Poincare sphere so that data from one polarization interferes with the other, i.e., crosstalk that results in confusion of X symbols with Y symbols, and vice versa. It is shown as well that allowing higher SNR penalty has lesser effect on SOP tracking.

6.4. RLS, NLMS, LMS, and MMA in Presence of Colored Noise. In this subsection, we compare floating-point MMA, LMS, NLMS, and RLS algorithms in terms of both convergence speed and steady state performance. In comparison to wireless, SOP transients in a MIMO system are unique to optical fiber communication, and it does cause the channel response to become nonstationary. PDL can be compared to slow fading; while combined with SOP transient, it becomes more like "short-duration statistically nonstationary fast-fading channel." The authors in [53] performed a detailed study comparing RLS, LMS, and sign updating algorithms in time-varying channels. It shows RLS outperforms other methods in term of excess mean-square estimation error, unless the eigenvalues of the input signals covariance matrix are equal. The later condition is not the case in presence of PDL. In [54–56], authors compared RLS and LMS in wireless context with time-varying nonstationary channels. It was shown that depending on the SNR and channel bandwidth, LMS can have a better performance with chirp-like signals. In [57], the authors introduced a whitening process that can be applied after the adaptive filters to improve coherent receivers' performance in the presence of PDL. Our simulations showed that with slow variation of SOP, applying the whitening matrix prior to decision block helped reducing ROSNR. However, in the presence of fast SOP fluctuation, updating the whitening matrix as quickly is challenging in practice.

Convergence speed of adaptive filters is part of the signal acquisition process in coherent receivers. Acquisition time is a key specification in optical networks. Initialization needs to be performed each time the signal is rerouted or recovers from loss of signal. As an example of the stringent limitation on recovery time, SONET protection should recover within 50 ms as stated in the Telcordia© GR-253-Core specification [58]. In [59], it is discussed that for 5G networks, the "0-Switching time" is as low as 1 ms, and latency is 10x better compared to previous wireless network generations. Since the wireless networks depend heavily on optical links for their backbone connections, that imposes severe requirements on the design of the next generation coherent

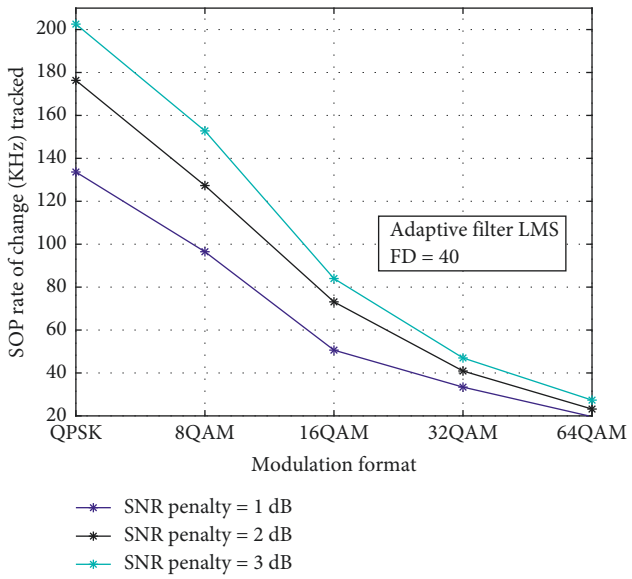

Figure 6: SOP tracking versus modulation format for different SNR penalties.

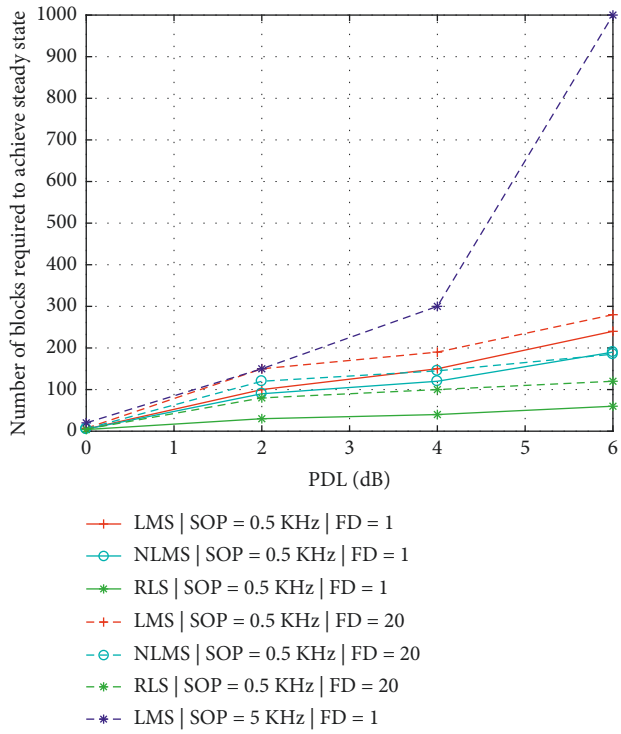

Figure 7: Number of blocks required to reach steady state versus PDL using 16QAM.

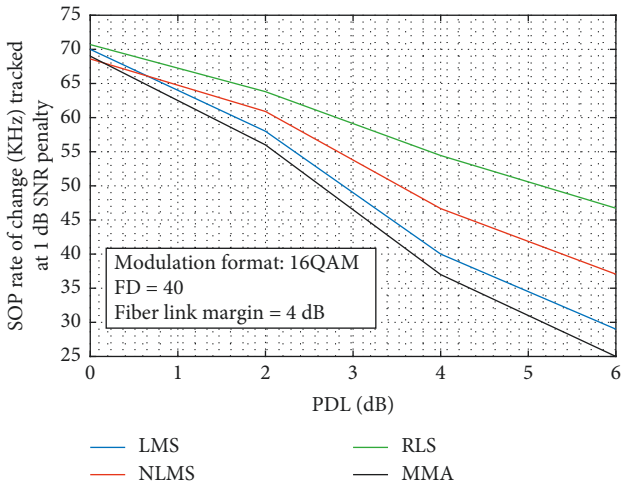

Figure 8: Achievable SOP tracking for 16QAM versus PDL.

transponders. In Figure 7, our Monte–Carlo simulation shows the number of blocks required for the system to reach convergence (bit error rate equivalent to steady state) as the function of PDL using 16QAM as modulation format, 0.15 for LMS gain and 0.985 as RLS forgotten factor, and "Link SNR Margin" of 4 dB. We can see, as expected, that RLS outperforms NLMS, which is faster than LMS. Although it is accepted to assume that acquisition is not performed under fast SOP transients, that is because the latter are supposed to be a rare event. However, we tested few cases with 5 kHz; we show that even with FD of 1, the high oscillatory behavior due to PDL and SOP results in long acquisition time. We can see how a FD of 20 blocks caused the acquisition time for RLS with PDL of 6 dB to double. As detailed in [60], even though RLS is significantly superior to LMS in terms of convergence performance, the tracking in nonstationary environments must be studied on case-by-case basis. For a fixed penalty of 1.0 dB from the theoretical ROSNR, we compare the three adaption methods when the signal is affected by PDL.

It is shown, in Figure 8, all four methods are tracking similar SOP rate of change transient when there is no PDL. As the latter increases, the 2×2 covariance matrix of the input signal used in RLS (P in equation (5) is an iterative estimate of the covariance matrix) or its trace used in NLMS (step size being normalized by the power of the input symbols) help with tracking SOP.

In case of LMS using a fixed step size, with PDL acting as random attenuators, the tracking capability is limited as no form of "power equalization" is performed. MMA is comparable to LMS in terms of implementation complexity; however, it can have a lower feedback delay. As expected, for same error signal feedback delay, the blind MMA is a bit noisier than decision-directed LMS, and hence the SOP tracking capability is lower.

7. Conclusions

First, we studied the performance of LMS adaptive filter, in the context of dual-polarization coherent optical receivers, in the presence of SOP transients, PDL, and ROADMs. The tradeoff between tracking capability and implementation noise when choosing the step size and forgetting factor is a key design decision, and we showed how the higher the step size the, more SOP tracking the adaptive filter will be handling but at the price of higher B2B/PDL ROSNR. The higher the order the modulation formats, the less tracking

can be done, and a reduction of 30% is expected for an increase of one bit per symbol. Error signal feedback delay is a key bottleneck for higher SOP tracking, and we showed due to higher BER oscillatory behavior that a delay of 40 blocks of 512 symbols can reduce tracking by 50% compared to FD of 20 blocks. As well, for each one dB PDL increase in link, the SOP tracking capability is reduced by 7.1 kHz and 8.6 kHz for SNR penalty of 1 and 2 dB, respectively. Finally, we presented the impact of concatenating ROADMs on SOP tracking. The RLS algorithm, using a covariance matrix as an aggressive dynamic "step size," has an advantage over the LMS and NLMS algorithms in both convergence speed and tracking in steady state in presence of PDL (and other colored noise) in the fiber. Our simulation data showed that RLS is ~2.5x faster than LMS when comparing convergence speed at 6 dB PDL with fast and slow SOP rotations. NLMS, using the trace of the covariance matrix, is around 2x slower than RLS. For SOP tracking, all studied algorithms have similar performance without the presence of colored noise. Otherwise, RLS outperforms both NLMS and LMS. On the other hand, RLS complexity growth, as a function of filter length, is quadratic $O(L^2)$, unlike LMS and MMA where complexity increases in a linear fashion. The length of the filter governs how much PMD the receiver is designed to compensate for. It is worth noting that choosing one of the algorithms depends on the application. For example, the case of Data Center Interconnect (DCI) of 100 KMs will not have considerable PDL in the link, and the requirement for low power consumption is rigid; therefore, LMS or MMA can be a good choice.

Data Availability

The simulation data used to support the findings of this study are included within the article.

Disclosure

In [6], the authors studied the tracking performance of LMS-adaptive algorithm with QPSK modulation format, operating at 100 Gb/s line rate, in the presence of fast SOP and PDL. In [61], the authors looked at only LMS algorithm in flexible data-rate coherent transceivers.

Conflicts of Interest

The authors declare that they have no conflicts of interest.

Acknowledgments

The authors acknowledge the support of the Natural Sciences and Engineering Research Council of Canada (NSERC).

References

[1] S. Jansen, I. Morita, and H. Tanaka, "16 × 52.5-Gb/s, 50-GHz Spaced, POLMUX-CO-OFDM transmission over 4,160 Km of SSMF enabled by MIMO processing," in *Proceedings of the 33rd European Conference and Exhibition of Optical Communication-Post-Deadline Papers 2007*, ECOC, Berlin, Germany, September 2007.

[2] A. N. Kolmogorov, "Interpolation and extrapolation of stationary random sequences," *The USSR Science Academic Bulletin*, vol. 5, 1941.

[3] N. Wiener, *The Extrapolation, Interpolation and Smoothing of Stationary Time Series*, MIT Press, Cambridge, MA, USA, 1942.

[4] B. Widrow, J. McCool, and M. Ball, "The complex LMS algorithm," *Proceedings of the IEEE*, vol. 63, no. 4, 1975.

[5] A. J. van der Veen and A. Paulraj, "An analytical constant modulus algorithm," *IEEE Transactions on Signal Processing*, vol. 44, no. 5, pp. 1136–1155, 1996.

[6] A. Abdo and C. D'Amours, "Performance of LMS based adaptive filtering in coherent optical receivers in presence of state-of-polarization transients, PDL and ROADMs," in *2018 IEEE Canadian Conference on Electrical & Computer Engineering (CCECE)*, pp. 1–4, Quebec City, Canada, May 2018.

[7] IEEE Standard, "IEEE guide for improving the lightning performance of electric power overhead distribution lines," Report, IEEE Standard 1410, New York, NY, USA, 1997.

[8] E. Collett, *Polarized Light: Fundamentals and Applications (Optical Engineering, Vol 36)*, CRC Press, Boca Raton, FL, USA, 1st edition, 1993.

[9] T. Brugière, T. H.R. Crawford, A. Mortelette et al., "Polarization activity monitoring of an aerial fiber link in a live network," in *Proceedings of the Optical Fiber Communication Conference (OFC)*, pp. 1–3, Anaheim, CA, USA, March 2016.

[10] L. E. Nelson, M. Birk, S. L. Woodward, and P. Magill, "Field measurements of polarization transients on a long-haul terrestrial link," in *Proceedings of the IEEE Photonic Society 24th Annual Meeting*, pp. 833-834, Arlington, VA, USA, December 2011.

[11] D. Charlton, S. Clarke, D. Doucet et al., "Field measurements of SOP transients in OPGW, with time and location correlation to lightning strikes," *Optics Express*, vol. 25, no. 9, pp. 9689–9696, 2017.

[12] S. M. Pietralunga, J. Colombelli, A. Fellegara, and M. Martinelli, "Fast polarization effects in optical aerial cables caused by lightning and impulse current," *IEEE Photonics Technology Letters*, vol. 16, no. 11, pp. 2583–2585, 2004.

[13] F. Pittalà, C. Stone, D. Clark, M. Kuschnerov, C. Xie, and A. Haddad, "Laboratory measurements of SOP transients due to lightning strikes on OPGW cables," in *Proceedings of the Optical Fiber Communication Conference (OFC)*, San Diego, CA, USA, March 2018.

[14] J. Wuttke, P. M. Krummrich, and J. Rosch, "Polarization oscillations in aerial fiber caused by wind and power-line current," *IEEE Photonics Technology Letters*, vol. 15, no. 6, pp. 882–884, 2003.

[15] Y. Namihira, Y. Horiuchi, S. Ryu, K. Mochizuki, and H. Wakabayashi, "Dynamic polarization fluctuation characteristics of optical fiber submarine cables under various environmental conditions," *Journal of Lightwave Technology*, vol. 6, no. 5, pp. 728–738, 1988.

[16] O. Karlsson, J. Brentel, and P. A. Andrekson, "Long-term measurement of PMD and polarization drift in installed fibers," *Journal of Lightwave Technology*, vol. 18, no. 7, pp. 941–951, 2000.

[17] T. Geisler and P. Kristensen, "Polarization properties of DCMs: thermal variations," in *Proceedings of Optical Fiber Communication Conference*, pp. 1–3, San Diego, CA, USA, March 2009.

[18] T. Geisler, M. N. Andersen, and T. Tokle, "Reduction of fast SOP changes in DSCMs under influence of shock and vibrations," in *Proceedings of the 2010 Conference on Optical Fiber Communication*, pp. 1–3, San Diego, CA, USA, March 2010.

[19] S. Han, M. Vanleeuwen, V. Dangui et al., "System penalty in coherent receiver considering distributed PMD, PDL, and ASE," *IEEE Photonics Technology Letters*, vol. 25, no. 9, pp. 885–887, 2013.

[20] E. Awwad, Y. Jaouën, and G. R.-B. Othman, "Polarization-time coding for PDL mitigation in long-haul PolMux OFDM systems," *Optics Express*, vol. 21, no. 19, p. 22773, 2013.

[21] T. Pfau, M. El-Darawy, C. Wordehoff et al., "32-krad/s polarization and 3-dB PDL tracking in a real-time digital coherent polarization-multiplexed QPSK receiver," in *Proceedings of the IEEE/LEOS Summer Topical Meetings*, Acapulco, Mexico, July 2008.

[22] S. O. Arik, J. M. Kahn, and K.-P. Ho, "MIMO signal processing for mode-division multiplexing: an overview of channel models and signal processing architectures," *IEEE Signal Processing Magazine*, vol. 31, no. 2, pp. 25–34, 2014.

[23] Q. Guo, B. Xu, and K. Qiu, "Studies on effects of feedback delay on the convergence performance of adaptive time-domain equalizers for fiber dispersive channels," *Optical Engineering*, vol. 55, no. 4, Article ID 046110, 2016.

[24] P. K. Meher et al., "Low adaptation-delay LMS adaptive filter part-I: introducing a novel multiplication cell," in *Proceedings of the 2011 IEEE 54th International Midwest Symposium on Circuits and Systems*, pp. 1–4, Seoul, South Korea, August 2011.

[25] Y. Feng, L. Li, J. Lin et al., "Joint tracking and equalization scheme for multi-polarization effects in coherent optical communication systems," *Optics Express*, vol. 24, no. 22, pp. 25491–25501, 2016.

[26] D. Chu, "Polyphase codes with good periodic correlation properties (Corresp.)," *IEEE Transactions on Information Theory*, vol. 18, no. 4, pp. 531-532, 1972.

[27] M. Noelle, R. Elschner, F. Frey, C. Schmidt-Langhorst, J. K. Fischer, and C. Schubert, "Performance of CAZAC training sequences in data-aided single-carrier optical transmission systems," in *Proceedings of the Photonic Networks; 16. ITG Symposium*, pp. 1–6, Leipzig, Germany, May 2015.

[28] C. Zhu, A. V. Tran, C. D. Cuong, S. Chen, T. Anderson, and E. Skafidas, "Digital signal processing for training-aided coherent optical single carrier frequency-domain equalization systems," *Journal of Lightwave Technology*, vol. 32, no. 24, pp. 4712–4722, 2014.

[29] F. Pittala, I. Slim, A. Mezghani, and J. A. Nossek, "Training-aided frequency-domain channel estimation and equalization for single-carrier coherent optical transmission systems," *Journal of Lightwave Technology*, vol. 32, no. 24, pp. 4849–4863, 2014.

[30] M. Kuschnerov, M. Chouayakh, K. Piyawanno et al., "Data-aided versus blind single-carrier coherent receivers," *IEEE Photonics Journal*, vol. 2, no. 3, pp. 387–403, 2010.

[31] O. Gerstel, M. Jinno, A. Lord, and S. J. Yoo, "Elastic optical networking: a new dawn for the optical layer?," *IEEE Communications Magazine*, vol. 50, no. 2, pp. s12–s20, 2012.

[32] A. Mitra, A. Lord, S. Kar, and P. Wright, "Effect of link margin and frequency granularity on the performance of a flexgrid optical network," in *Proceedings of the 39th European Conference and Exhibition on Optical Communication*, London, UK, September 2013.

[33] F. Buchali, A. Klekamp, L. Schmalen, and T. Drenski, "Implementation of 64QAM at 42.66 GBaud using 1.5 samples per symbol DAC and demonstration of up to 300 km fiber transmission," in *Proceedings of the Optical Fiber Communication Conference*, San Francisco, CA, USA, March 2014.

[34] A. Souari, M. L. Ammari, A. Gawanmeh, and S. Tahar, "Performance evaluation of time and frequency domain equalizers," in *Proceedings of the Canadian Conference on Electrical and Computer Engineering (CCECE)*, pp. 1–6, Toronto, ON, USA, May 2014.

[35] A. Mecozzi and M. Shtaif, "The statistics of polarization-dependent loss in optical communication systems," *IEEE Photonics Technology Letters*, vol. 14, no. 3, pp. 313–315, 2002.

[36] X. Zhou and C. Xie, *Enabling Technologies for High Spectral-Efficiency Coherent Optical Communication Networks*, Wiley, Hoboken, NJ, USA, 2016.

[37] T. Kimijima, K. Nishikawa, and H. Kiya, "A pipelined architecture for DLMS algorithm considering both hardware complexity and output latency," in *Proceedings of the 9th European Signal Processing Conference*, pp. 1–4, Rhodes, Greece, September 1998.

[38] E. P. da Silva and D. Zibar, "Widely linear equalization for IQ imbalance and skew compensation in optical coherent receivers," *Journal of Lightwave Technology*, vol. 34, no. 15, pp. 3577–3586, 2016.

[39] M. Paskov, D. Lavery, and S. J. Savory, "Blind equalization of receiver in-phase/quadrature skew in the presence of nyquist filtering," *IEEE Photonics Technology Letters*, vol. 25, no. 24, pp. 2446–2449, 2013.

[40] J. G. Proakis, *Digital Communications*, McGraw-Hill International, New York, NY, USA, 4th edition, 2001.

[41] T. A. Strasser and J. L. Wagener, "Wavelength-selective switches for ROADM applications," *IEEE Journal of Selected Topics in Quantum Electronics*, vol. 16, no. 5, pp. 1150–1157, 2010.

[42] H. Simon, *Adaptive Filter Theory*, Prentice-Hall, New Jersey, NJ, USA, 4th edition, 2002.

[43] G. Long, F. Ling, and J. G. Proakis, "The LMS algorithm with delayed coefficient adaptation," *IEEE Transactions on Acoustic, Speech, and Signal Processing*, vol. 37, no. 9, pp. 1397–1405, 1971.

[44] O. Ishida, K. Takei, and E. Yamazaki, "Power efficient DSP implementation for 100G-and-beyond multi-haul coherent fiber-optic communications," in *Proceedings of the 2016 Optical Fiber Communications Conference*, pp. 1–3, Anaheim, CA, USA, March 2016.

[45] Socionext, "100 g to 400 g Adc and Dac for ultra-high-speed optical networks," August 2018, http://socionextus.com/products/networking-asic/adc-dac/.

[46] C. Schmidt, C. Kottke, R. Freund, F. Gerfers, and V. Jungnickel, "Digital-to-analog converters for high-speed optical communications using frequency interleaving: Impairments and characteristics," *Optics Express*, vol. 26, no. 6, pp. 6758–6770, 2018.

[47] W. C. Ng, A. T. Nguyen, C. S. Park, and L. A. Rusch, "Reduction of MIMO-FIR taps via SOP-estimation in Stokes space for 100 Gbps short reach applications," in *Proceedings of the European Conference on Optical Communication (ECOC)*, pp. 1–3, Cannes, France, September 2014.

[48] R. H. Kwong and E. W. Johnston, "A variable step size LMS algorithm," *IEEE Transactions on Signal Processing*, vol. 40, no. 7, pp. 1633–1642, 1992.

[49] R. Harris, D. Chabries, and F. Bishop, "A variable step (VS) adaptive filter algorithm," *IEEE Transactions on Acoustics,*

Speech, and Signal Processing, vol. 34, no. 2, pp. 309–316, April 1986.

[50] Cisco Systems, *Cisco Transport Planner DWDM Operations Guide Release 9.0*, Cisco Systems, San Jose, CA, USA, 2015.

[51] A. Ghosh, *Fundamentals of LTE*, Prentice Hall Press, Upper Saddle River, NJ, USA, 2010.

[52] C. C. Chan, *Optical Performance Monitoring: Advanced Techniques for Next-Generation Photonic Networks*, Elsevier, New York, NY, USA, 2010.

[53] E. Eweda, "Comparison of RLS, LMS, and sign algorithms for tracking randomly time-varying channels," *IEEE Transactions on Signal Processing*, vol. 42, no. 2, 1994.

[54] P. C. Wei, J. Han, J. R. Zeidler, and W. H. Ku, "Comparative tracking performance of the LMS and RLS algorithms for chirped narrowband signal recovery," *IEEE Transactions on Signal Processing*, vol. 50, no. 7, pp. 1602–1609, 2002.

[55] O. Macchi, N. Bershad, and M. Mboup, "Steady-state superiority of LMS over LS for time-varying line enhancer in noisy environment," *IEE Proceedings F Radar and Signal Processing*, vol. 138, no. 4, pp. 354–360, 1991.

[56] P. Lin, P. Rapajic, and Z. Krusevac, "On the tracking performance of LMS and RLS algorithms in an adaptive MMSE CDMA receiver," in *Proceedings of the Australian Communications Theory Workshop ACTW*, pp. 175–178, Brisbane, Australia, February 2005.

[57] M. Zamani, Z. Zhang, C. Chen, and C. Li, "PDL compensation using whitening matrix in polarization division multiplexed coherent optical transmission," in *Proceedings of the Optical Fiber Communication Conference (OFC)*, Anaheim, CA, USA, March 2013.

[58] GR-253-Core, "Telcordia GR-253—documentation information," August 2018, https://telecom-info.telcordia.com/ido/AUX/GR_253_TOC.i03.pdf.

[59] I. Parvez, A. Rahmati, I. Guvenc, A. I. Sarwat, and H. Dai, "A Survey on low latency towards 5G: RAN, core network and caching solutions," *IEEE Communications Surveys and Tutorials*, vol. 20, no. 4, pp. 3098–3130, 2017.

[60] A. H. Sayed, *Fundamentals of Adaptive Filtering*, Wiley & Sons, Inc., Hoboken, NJ, USA, 1st edition, 2003.

[61] A. Abdo and C. D'Amours, "Tracking capability of adaptive LMS algorithm in coherent optical flexible-rate transceivers," in *Proceedings of the 2019 Photonics North (PN)*, Quebec City, Canada, May 2019.